Role and mechanism of miR-130a-3p in the chemosensitivity of retinoblastoma cells to vincristine

Xiulan Lu
Tianjin Medical University Eye Hospital
Huifang Tu
Wuhan Aier Eye Hospital
Dongrun Tang
Tianjin Medical University Eye Hospital
Xiaoming Huang
Tianjin Medical University Eye Hospital
Fengyuan Sun (drsunfengyuan1231@163.com)
Tianjin Medical University Eye Hospital https://orcid.org/0000-0003-3201-7678

Research Article

Keywords: miR-130a-3p, PAX6, Retinoblastoma, Proliferation, Chemosensitivity, Resistance index, Post-transcriptional regulation

Posted Date: July 26th, 2021

DOI: https://doi.org/10.21203/rs.3.rs-545641/v1

Abstract

Purpose

Chemoresistance remains the primary obstacle threatening the prognosis of retinoblastoma (RB). microRNAs (miRNAs) are acknowledged as critical regulator of drug resistance. This study explored the molecular mechanism of miR-130a-3p affecting the chemosensitivity of RB to vincristine (VCR).

Methods

miR-130a-3p expression of VCR-sensitive and VCR-resistant RB tissues was detected using RT-qPCR. VCR-resistant RB cell line Y79/VCR was induced. miR-130a-3p expression of Y79/VCR cell line and its corresponding parental cell line was detected. Y79/VCR cells were subjected to miR-130a-3p overexpression treatment. The cell proliferation was measured using MTT assay, and the IC50 value and drug resistance index were examined using CCK-8 assay. The targeting relationship between miR-130a-3p and PAX6 was predicted through bioinformatics analysis and verified using dual-luciferase assay. Functional rescue experiments were conducted to confirm the role of PAX6 in chemosensitivity of RB cells. The effect of miR-130a-3p on tumorigenesis and VCR sensitivity was observed *in vivo*.

Results

miR-130a-3p was downregulated in VCR-resistant RB tissues and cells. Overexpression of miR-130a-3p repressed the proliferation of VCR-resistant RB cells and enhanced chemosensitivity. miR-130a-3p targeted PAX6 expression. Overexpression of PAX6 reversed the effect of miR-130a-3p on chemosensitivity of RB. Overexpression of miR-130a-3p suppressed tumor growth and reduced VCR resistance *in vivo*.

Conclusion

miR-130a-3p enhanced the chemosensitivity of RB cells to VCR by targeting PAX6 expression.

Introduction

Retinoblastoma (RB) represents a primary intraocular malignancy commonly in children under 5 years old [1]. Most RB in one or both eyes is resulted from biallelic mutation of the RB suppressor gene (RB1) in immature retinal cells [2]. In clinical, RB is often manifested as leukocoria, and the patients may also present strabismus, misalignment of the eyes, and vision decline [3]. The available treatments include chemotherapy, radiotherapy, enucleation, as well as focal treatments including cryotherapy, transpupillary thermotherapy, and laser photocoagulation [4]. Chemotherapy is currently recognized as the first-line treatment for RB in children and the chemotherapeutic agents can be delivered through intravenous, intra-

arterial, periocular, and intravitreal injection [5]. At present, vincristine (VCR) constitutes one of the standard chemotherapeutic agents applied for RB [6]. However, the clinical application of chemotherapeutic agents is severely limited due to inherent or acquired resistance, eventually leading to unfavorable outcome and poor survival [7]. Thus, elucidating the mechanisms of chemoresistance and improving the therapy response have significant implications for RB patients.

microRNAs (miRNAs) are a class of small endogenous non-coding RNAs (18–25 nt in length), participating in the modulation of gene expressions at the post-transcriptional level and negatively modulating the expression of tumor-associated molecules [8]. Dysregulated miRNAs are implicated in tumorigenesis, progression, and prognosis, and also miRNAs are prospective targets contributing to improving the diagnosis and prognosis prediction and enhancing the chemotherapy response [9]. It is well established that aberrant miRNA expression serves as the intervention target for the resistance of RB cells to chemotherapeutic agents [10–12]. miR-130a-3p is identified to be a tumor suppressor in various malignancies, such as breast cancer [13], lung cancer [14], and gastric cancer [15]. However, the role of miR-130a-3p in RB has not been studied before. Importantly, emerging evidence has revealed that miR-130a-3p plays a vital role in tumor chemoresistance [16–19]. For example, Hu et al. have demonstrated that miR-130a-3p is downregulated in cisplatin-resistant non-small cell lung cancer cells, and miR-130a-3p inhibition contributes to cisplatin resistance [18]. Asukai et al. have shown that miR-130a-3p regulates gemcitabine resistance in cholangiocarcinoma via PPARG [20]. Accordingly, we speculated that miR-130a-3p can regulate the sensitivity of RB to VCR through post-transcriptional regulation of target genes. This study herein sought to investigate the molecular mechanism of miR-130a-3p affecting the chemosensitivity of RB to VCR, which shall confer novel insights for the improvement of chemotherapeutic effect in RB patients.

Materials And Methods

Clinical sample

Tissue samples were collected from 34 RB patients for extirpation operation in Tianjin Medical University Eye Hospital from June 2019 to June 2020, aged 10–37 months (2.28 ± 0.58 years). All RB patients received VCR chemotherapy before operation, but did not receive radiotherapy. According to the recurrence time, they were allocated into two groups: 21 patients in the VCR-sensitive group (within 6 months) and 13 patients in the VCR-resistant group (over 6 months). The normal retinal tissues were collected from 13 patients with eyeball rupture as the control. The tissue samples were washed with phosphate-buffered saline (PBS), frozen overnight in liquid nitrogen, and then stored at -80℃.

Construction, culture and transfection of VCR-resistant RB cell line

RB cell lines (Y79, WERI-Rb-1, SO-Rb50, and SO-Rb70) were obtained from National Infrastructure of Cell Line Resource (www.cellresource), and human retinal astrocyte (HRA) was purchased from ZQXZ Biotech

(Shanghai, China). All the cells were cultured in RPMI-1640 medium (Sigma-Aldrich, Merck KGaA, Darmstadt, Germany) containing 10% fetal bovine serum (FBS) and 1% penicillin-streptomycin-glutamine (100X, Gibco, Grand Island, NY, USA) at 37℃ with 5% CO_2 [21]. The VCR-resistant RB cell line was constructed by E-test, lasting for 9 months, and the concentration of VCR ranged from 75 μg/mL to 600 μg/mL. Then the cells were maintained for 2 weeks without VCR. The 50% inhibiting concentration (IC50) was determined using cell counting kit-8 (CCK-8) assay [7].

Y79/VCR cells in logarithmic growth phase were seeded into 6-well plates (4×10^5 cells/well). Upon reaching 70–80% confluence, the cells were transfected with mimic-NC, miR-130a-3p mimic, PAX6 overexpression plasmid, and its NC plasmid (Genechem Co., Ltd, Shanghai, China) in line with the instructions of Lipofectamin 2000 (11668-019, Invitrogen, Calsbad, CA, USA). Briefly, 10 μg plasmids (the final concentration was 50 nM) diluted by 250 μL serum-free Opti-MEM were fully mixed with 5 μL Lipofectamin 2000 diluted by 250 μL serum-free Opti-MEM. After standing for 20 min, the mixture was added to the 6-well plates. The transfected cells were cultured under the conditions of 37℃, 5% CO_2, and saturation humidity. After 48 h, the medium containing transfection reagent was replaced by RPMI-1640 medium containing 10% FBS for another 24–48 h incubation.

3-(4,5-dimethylthiazol-2-yl)-2,5-diphenyltetrazolium bromide (MTT) assay

Y79/VCR cells were seeded into 96-well plates (1×10^4 cells/well). After 24, 48, and 72 h-incubation, the cells were supplemented with 20 μL MTT solution (Sigma-Aldrich) and cultured for 4 h in a humidified incubator. After the supernatant was removed, 200 μL dimethyl sulfoxide (DMSO) was added to each well. The absorbance at 490 nm was measured by a microplate reader (Bio-Rad, Hercules, CA, USA) [22].

CCK-8 assay

The transfected Y79/VCR cells were seeded into 96-well plates (1500 cells/well) and cultured for 6 days. The cells were cultured in VCR medium of different concentrations (100 μg/mL, 200 μg/mL, 400 μg/mL, and 600 μg/mL) for 48 h. Then each well was supplemented with 20 mL CCK-8 solution (5 mg/mL) for another 4 h-incubation. The crystal was dissolved by 100 mL DMSO. The absorbance at 570 nm was measured by a microplate reader (Bio-Rad). The IC50 of VCR was calculated, and finally the resistance index (RI) was obtained: RI = IC50 (drug-resistant strain)/IC50 (parental strain) [23].

Reverse transcription quantitative polymerase chain reaction (RT-qPCR)

Total RNA was extracted from tissues and cells using TRIzol (Invitrogen), and the concentration and purity of RNA were detected using ultraviolet spectrophotometer (1011U, NanoDrop Technologies Inc., Wilmington, DE, USA). The cDNA was generated according to the instructions of TaqMan MicroRNA Assays Reverse Transcription primer (4427975, Applied Biosystems, Inc., Carlsbad, CA, USA). The primers of miR-130a-3p and PAX6 were designed and synthesized by Takara (Dalian, China) (Table 1). RT-qPCR

was performed on ABI7500 qPCR instrument (ABI, Foster City, CA, USA). The reaction conditions were pre-denaturation at 95℃ for 10 min, denaturation at 95℃ for 10 s, annealing at 60℃ for 20 s, and extension at 72℃ for 34 s, a total of 40 cycles. The relative expression of genes was examined by $2^{-\Delta\Delta Ct}$ method, with GAPDH or U6 as the internal reference. The experiment was repeated 3 times.

Table 1
Primer sequence for RT-qPCR

Name of primer	Sequences
miR-130a-3p	F: 5'-CGCCGCAGTGCAATGTTAAA-3'
	R: 5'-GTGCAGGGTCCGAGGTATTC-3'
U6	F: 5'-GCTTCGGCAGCACATATACT-3'
	R: 5'-GTGCAGGGTCCGAGGTATTC-3'
PAX6	F: 5'-AGACACAGCCCTCACAAAC-3'
	R: 5'-ATCATAACTCCGCCCATTC-3'
GAPDH	F: 5'-CCACCCAGAAGACTGTGGAT-3'
	R: 5'-TTCAGCTCAGGGATGACCTT-3'

Western blot

The tissues were placed in centrifuge tubes and added with 500 μL radio-immunoprecipitation assay cell lysate (R0020, Solarbio, Beijing, China) (containing 1 mmol/L phenylmethylsulfonyl fluoride). The tissues were homogenized at 1000 g until fully lysis. The homogenate was placed on ice for 30 min and then centrifuged at 4℃ and 12000 g for 4 min, and the supernatant was collected and stored at -80℃. The protein concentration was determined using bicinchoninic acid kit (AR0146, Boster, Wuhan, Hubei, China), and the concentration of each sample was adjusted to 3 μg/μL. The extracted protein was added with the loading buffer and boiled at 95℃ for 10 min. Equal amount of protein on each lane (30 μg) was separated on 10% SDS-polyacrylamide gel and transferred onto polyvinylidene fluoride membranes (P2438, Sigma-Aldrich). The membranes were blocked with 5% bovine serum albumin (10-L16, Biopartner Science & Technology, Beijing, China) for 1 h and cultured with the primary antibody rabbit anti-PAX6 (ab195045, 1:1000, Abcam Inc., Cambridge, MA, USA) at 4℃ overnight. Following tris-buffered saline-tween (TBST) buffer washing (3 times × 5 min), the membranes were cultured with the secondary antibody (ab6721, 1:2000, Abcam) for 1 h. Following TBST washing (3 times × 5 min), the bands were developed with enhanced chemiluminescence reagent. The gray level of each band was analyzed using Image J 1.48 (Media Cybernetics, Bethesda, MA, USA), with GADPH (ab181602, 1:10000, Abcam) as internal reference.

Dual-luciferase assay

The target site sequence (WT) of PAX6 mRNA 3'-UTR region and the sequence after the mutation of WT target site (MUT) were synthesized. The pmiR-RB-REPORT™ plasmid was subjected to restriction enzyme digestion, and then the synthetic target gene fragments WT and MUT were inserted into pmiR-RB-REPORT™, respectively. The constructed WT and MUT vectors were transfected with mimic-NC or miR-130a-3p mimic into 293T cells (CRL-3216, American Type Culture Collection, Manassas, Virginia, USA). The cells were collected and lysed 48 h after transfection. The relative activity of luciferase was detected using dual-luciferase detection kit (RG005, Beyotime, Shanghai, China). The experiment was repeated 3 times.

Xenograft tumor in nude mice

Thirty-two BALB/c nude mice (aged 4–6 weeks and weighing 16-20g) were raised in laminar flow cabinet (specific pathogen grade) and exposed to ultraviolet light at regular intervals. Cages, rubbish, drinking water, and feed were sterilized. The room temperature was maintained at 24℃-26℃, and the relative humidity was maintained at 40%-60%. Y79 or Y79/VCR cells were mixed with PBS respectively to prepare single cell suspension (1×10^6 cells/mL), and then 50 μL cell suspension was subcutaneously injected into the right side of each nude mouse. After 1 week, the mice were randomly allocated into four groups (N = 8): Y79 group, Y79/VCR group, Y79/VCR + agomiR-NC group, and Y79/VCR + agomiR-130a-3p group. After that, agomiR-NC and miR-130a-3p agomiR were injected into the tumor site respectively. All the mice received intraperitoneal injection of VCR (0.5 mg/kg) for 5 weeks, once a week. The tumor growth was measured with vernier caliper every week. The tumor volume was calculated as follows: $V = (L \times W^2)/2$. After 5 weeks, the mice were euthanized with 100 mg/kg pentobarbital sodium (P3761, Sigma-Aldrich). The xenograft tumors were resected and weighed.

Immunohistochemistry

The weighed tumor tissues were prepared into paraffin sections, dewaxed, dehydrated with gradient alcohol, and washed with tap water for 2 min. Then the sections were treated with 3% methanol containing H_2O_2 for 20 min, and washed with distilled water for 2 min and 0.1 M PBS for 3 min. The tissue sections were treated with antigen repair solution and cooled by tap water. The sections were blocked with normal goat serum sealing solution (C-0005, Haoran Bio Technologies Co., Ltd, Shanghai, China) for 20 min, and then incubated with the primary antibody PAX6 (ab195045, 1:500, Abcam) at 4℃ overnight. Following 0.1 M PBS washing (3 times × 5 min), the sections were incubated with the horseradish peroxidase-labeled streptomyces ovalbumin working solution (0343-10000U, Imunbio Biotechnology Co., Ltd, Beijing, China) at 37℃ for 20 min. Afterward, the sections were developed with 2,4-diaminobutyric acid (ST033, Whiga Technology Co., Ltd, Guangzhou, Guangdong, China), counterstained with hematoxylin (PT001, Bogoo Biological Technology Co., Ltd., Shanghai, China) for 1 min, and treated with 1% ammonia. Finally, the sections were dehydrated with gradient alcohol, cleared with xylene, and sealed with neutral resin, followed by observation under the microscope. Five fields were randomly selected from each section, and the number of positive cells in each field was counted [24].

Statistical analysis

Data analysis was introduced using the SPSS 21.0 (IBM Corp., Armonk, NY, USA) and GraphPad Prism 8.0 (GraphPad Software Inc., San Diego, CA, USA). Data are expressed as mean ± standard deviation. The unpaired *t* test was used for comparison between two groups. One-way analysis of variance (ANOVA) was employed for the comparisons among multiple groups, followed by Tukey's multiple comparisons test. Repeated measure ANOVA was employed for the comparisons between groups at different time points. The $p < 0.05$ indicated a significant difference.

Results

miR-130a-3p was downregulated in VCR-resistant RB tissues and cells

miR-130a-3p is downregulated in renal cell carcinoma, breast cancer, and liver cancer [25–27], but its role in RB remains unknown. miR-130a-3p expression in RB tissues and normal retinal tissues was detected using RT-qPCR, and the results demonstrated that miR-130a-3p expression of RB tissues was significantly lower than that of normal retinal tissues (Fig. 1A). All RB patients received VCR chemotherapy before operation. According to the recurrence time, the RB patients were allocated into VCR-sensitive group and VCR-resistant group. RT-qPCR results showed that compared with the VCR-sensitive group, the VCR-resistant group had reduced miR-130a-3p expression (Fig. 1B).

Moreover, compared with HRA cells, miR-130a-3p was poorly expressed in RB cell lines (Y79, WERI-Rb-1, SO-Rb50, and SO-Rb70), with Y79 cells showing the lowest expression (Fig. 1C). Then RB cell lines were subjected to VCR treatment, and the IC50 value was measured using CCK-8 assay to reflect the drug resistance of cells. The IC50 value of Y79 cells was the highest after VCR treatment (Fig. 1D), indicating that Y79 cells were the most resistant to VCR. Hence, we chose Y79 cell line for the follow-up experiments. We further detected miR-130a-3p expression of VCR-resistant cells (Y79/VCR) and its corresponding parental cells (Y79). The results revealed that miR-130a-3p expression in Y79/VCR cells was notably lower than that in parental cells (Fig. 1E) (all $p < 0.05$). Taken together, miR-130a-3p was downregulated in VCR-resistant RB tissues and cells.

Overexpression of miR-130a-3p repressed the proliferation of VCR-resistant RB cells and enhanced chemosensitivity

To investigate the effect of miR-130a-3p on VCR-resistant RB cells, we overexpressed miR-130a-3p in Y79/VCR cells. The transfection efficiency was verified using RT-qPCR (Fig. 2A). MTT assay showed that compared with that in the mimic-NC group, the cell proliferation in the miR-130a-3p mimic group was notably decreased (Fig. 2B) ($p < 0.05$). CCK-8 assay demonstrated that compared with that in the mimic-NC group, the IC50 value and drug RI of cells in the miR-130a-3p mimic group were notably reduced (Fig. 2C-D) ($p < 0.05$). Briefly, overexpression of miR-130a-3p repressed the proliferation of VCR-resistant RB cells and enhanced chemosensitivity.

miR-130a-3p inhibited PAX6 expression by post transcriptional regulation

Targetscan website (http://targetscan.org/vert_71/) predicted that miR-130a-3p had a binding site with PAX6 (Fig. 3A). Dual-luciferase assay confirmed that miR-130a-3p could specifically bind PAX6 (Fig. 3B) (all $p < 0.05$). PAX6 facilitates RB growth and inhibits apoptosis [28, 29]. Hence, we speculated that miR-130a-3p affected the chemosensitivity of RB cells by targeting PAX6.

Compared with that in the normal retinal tissues, PAX6 expression in RB tissues was significantly elevated (Fig. 3C). PAX6 expression in the VCR-resistant group was notably higher than that in the VCR-sensitive group (Fig. 3D). PAX6 expression in Y79/VCR cells was also higher than that in parental cells (Fig. 3E). PAX6 expression in Y79/VCR cells after overexpression of miR-130a-3p was detected, and the results exhibited that compared with the mimic-NC group, the miR-130a-3p mimic group showed reduced PAX6 expression (Fig. 3F) (all $p < 0.05$). Briefly, miR-130a-3p targeted PAX6 expression in VCR-resistant RB cells.

Overexpression of PAX6 reversed the effect of miR-130a-3p on chemosensitivity of RB

To further determine whether miR-130a-3p affected the proliferation and chemosensitivity of RB cells by targeting PAX6, we conducted a functional rescue experiment. Compared with the mimic NC + oe-NC group, the miR-130a-3p mimic + oe-NC group showed significantly reduced cell proliferation; compared with the miR-130a-3p mimic + oe-NC group, the miR-130a-3p mimic + oe-PAX6 group had enhanced cell proliferation (Fig. 4A) ($p < 0.05$). After overexpression of miR-130a-3p, the IC50 value and drug RI of cells were decreased notably, while on this basis, overexpression of PAX6 increased the IC50 value and drug RI of cells (Fig. 4B-C) ($p < 0.05$). Taken together, overexpression of PAX6 reversed the promoting effect of miR-130a-3p on chemosensitivity of RB.

Overexpression of miR-130a-3p suppressed tumor growth and reduced VCR resistance in vivo

Y79 or Y79/VCR cells were injected subcutaneously into the right side of nude mice, and agomiR-NC and miR-130a-3p agomiR were injected into the tumor site respectively. When the tumor volume reached about 100 mm^3, the nude mice were treated with VCR. Compared with those of the Y79 group, the tumor volume and weight of the Y79/VCR group were notably increased; compared with those of the Y79/VCR + agomiR-NC group, the tumor volume and weight of the Y79/VCR + agomiR-130a-3p group were decreased (Fig. 5A-C) ($p < 0.05$). The positive expression rate of PAX6 was detected using immunohistochemistry. Compared with that of the Y79 group, the positive rate of PAX6 protein of the Y79/VCR group was reduced; compared with that of the Y79/VCR + agomiR-NC group, the positive rate of PAX6 protein of the Y79/VCR + agomiR-130a-3p group were decreased (Fig. 5D) ($p < 0.05$). In brief, overexpression of miR-130a-3p suppressed tumor growth and reduced VCR resistance *in vivo* by targeting PAX6 expression.

Discussion

Chemotherapeutic agents extensively used in the treatment of RB; however, one of the most salient problem is that patients are prone to develop drug resistance, resulting in chemotherapy failure [7]. miRNA has a role in gene silencing and translational repression by binding to target mRNAs, which is implicated in the chemoresistance of diverse malignancies [30]. This study demonstrated that overexpression of miR-130a-3p enhanced the chemosensitivity of RB to VCR by targeting PAX6 expression.

It is well established that dysregulation of miRNA contributes to the initiation and progression of tumors, and even the chemoresistance of tumors [9]. The used of miRNA mimics or antagomiRs to correct the expression of these dysregulated miRNAs can normalize the gene regulatory network and thereby make tumor cells sensitive to chemotherapy [31]. miR-130a-3p is identified as a tumor suppressor and frequently downregulated in variant malignancies, such as breast cancer [32], hepatocellular carcinoma [26], and renal cell carcinoma [27]. To our knowledge, we were the first to demonstrate that miR-130a-3p expression was reduced in RB tissues and cells. Notably, the role of miR-130a-3p in tumor chemoresistance has been well documented in recent literature. For example, miR-130a-3p is downregulated in gemcitabine-resistant hepatocellular carcinoma cells, and activation of miR-130a-3p contributes to the chemosensitivity of hepatocellular carcinoma cells [33]. Similarly, overexpression of miR-130a-3p reverses cisplatin resistance of clear cell renal cell carcinoma [27]. We further detected miR-130a-3p expression of VCR-resistant cells and its corresponding parental cells. Our results revealed that miR-130a-3p was downregulated in VCR-resistant RB tissues and cells. Then, Y79/VCR cells were subjected to miR-130a-3p overexpression treatment. The proliferation, IC50 value, and RI of VCR-resistant RB cells transfected with miR-130a-3p mimic were measured. The results revealed that overexpression of miR-130a-3p repressed the proliferation of VCR-resistant RB cells and enhanced chemosensitivity. Consistently, it is reported that upregulation of miR-130a-3p can repress the proliferation of breast cancer cells [32] and significantly strengthen the cell sensitivity to doxorubicin [34].

Subsequently, we sought to determine the target genes of miR-130a-3p in regulating the chemosensitivity of RB cells. Targetscan website (http://targetscan.org/vert_71/) predicted that miR-130a-3p had a binding site with PAX6, and dual-luciferase assay confirmed that miR-130a-3p could specifically bind PAX6. PAX6 is a transcription factor belonging to the PAX family, which plays a vital role in the development of eyes, pancreas, and central nervous system [35]. PAX6 functions as a critical modulator in the coordination and pattern formation essential for retinogenesis, as well as the development of other ocular tissues [36]. PAX6 mutation causes eye defects and neurological abnormalities associated with structural alterations in the brain [35]. Importantly, aberrant upregulation of PAX6 has been observed in RB, leading to the onset and progression of RB [28]. PAX6 silencing represses growth and facilitates apoptosis of cultured human RB cells [37]. Also, PAX6 is reported to regulate the chemoresistance of glioblastoma stem cells to temozolomide [38]. Consequently, we speculated that miR-130a-3p affected the chemosensitivity of RB cells by targeting PAX6. This study exhibited that PAX6 expression was significantly elevated in RB tissues compared with that in the normal retinal tissues. PAX6 expression in the VCR-resistant tissues

and cells was also notably upregulated. PAX6 expression was reduced in Y79/VCR cells transfected with miR-130a-3p mimic. Briefly, miR-130a-3p targeted PAX6 expression in VCR-resistant RB cells. Functional rescue experiments verified that overexpression of PAX6 attenuated the promoting effect of miR-130a-3p on the chemosensitivity of RB cells. Moreover, the murine model of RB was established and the model mice underwent VCR treatment. Our results confirmed that overexpression of miR-130a-3p suppressed tumor growth and reduced VCR resistance *in vivo* by targeting PAX6 expression.

To sum up, miR-130a-3p was downregulated in RB tissues and cells, and upregulation of miR-130a-3p contributed to enhancing the chemosensitivity of RB cells to VCR by targeting PAX6 expression. This study hinted the possibility of miR-130a-3p as a promising target for RB patients with chemoresistance and possessed certain significance for the improvement of clinical practice of chemotherapy. However, whether miR-130a-3p can be adopted as a breakthrough to improve sensitivity to VCR needs further verification. Additionally, whether other targets of miR-130a-3p participate in the mechanism of VCR resistance in RB remains unknown. The mechanism of other targets and downstream signaling pathway of miR-130a-3p in VCR resistance will be assessed in the future study.

Declarations

Acknowledgements

We thank all of members in our team for the excellent work.

Author contributions

The concept of the study was planned and discussed by all project members. XL and HT were responsible for the concept design and data collection. DT analyzed data. The manuscript was written by XH and critically revised by FS. All authors reviewed and approved the final version.

Funding

This research was supported by Tianjin Key Clinicial Discipline Construction Project (TJLCZDXKT005).

Compliance with ethical standards

Competing interests

The authors declare that they have no competing interests.

Ethics approval and consent to participate

This study got the approval of the Ethical Committee of Tianjin Medical University Eye Hospital. The guardians of the patients signed the informed consent in accordance with the *Declaration of Helsinki*. All experimental procedures were implemented on the ethical guidelines for the study of experimental pain in conscious animals.

References

1. Ortiz MV, Dunkel IJ. Retinoblastoma (2016) J Child Neurol 31(2):227–236
2. Soliman SE, Racher H, Zhang C, MacDonald H, Gallie BL (2017) Genetics and Molecular Diagnostics in Retinoblastoma–An Update. Asia Pac J Ophthalmol (Phila) 6(2):197–207
3. Gudiseva HV, Berry JL, Polski A, Tummina SJ, O'Brien JM. Next-Generation Technologies and Strategies for the Management of Retinoblastoma. Genes (Basel). 2019; 10(12)
4. Yanik O, Gunduz K, Yavuz K, Tacyildiz N, Unal E (2015) Chemotherapy in Retinoblastoma: Current Approaches. Turk J Ophthalmol 45(6):259–267
5. Kaliki S, Shields CL (2015) Retinoblastoma: achieving new standards with methods of chemotherapy. Indian J Ophthalmol 63(2):103–109
6. Shukla S, Srivastava A, Kumar S, Singh U, Goswami S, Chawla B, Bajaj MS, Kashyap S, Kaur J (2017) Expression of multidrug resistance proteins in retinoblastoma. Int J Ophthalmol 10(11):1655–1661
7. Zhao B, Li B, Liu Q, Gao F, Zhang Z, Bai H, Wang Y (2020) Effects of matrine on the proliferation and apoptosis of vincristine-resistant retinoblastoma cells. Exp Ther Med 20(3):2838–2844
8. Cai Z, Zhang F, Chen W, Zhang J, Li H (2019) miRNAs: A Promising Target in the Chemoresistance of Bladder Cancer. Onco Targets Ther 12:11805–11816
9. Caliskan M, Guler H, Bozok Cetintas V (2017) Current updates on microRNAs as regulators of chemoresistance. Biomed Pharmacother 95:1000–1012
10. Yang G, Fu Y, Lu X, Wang M, Dong H, Li Q (2019) miR34a regulates the chemosensitivity of retinoblastoma cells via modulation of MAGEA/p53 signaling. Int J Oncol 54(1):177–187
11. Li C, Zhao J, Sun W (2020) microRNA-222-Mediated VHL Downregulation Facilitates Retinoblastoma Chemoresistance by Increasing HIF1alpha Expression. Invest Ophthalmol Vis Sci 61(10):9
12. He TG, Xiao ZY, Xing YQ, Yang HJ, Qiu H, Chen JB. Tumor Suppressor miR-184 Enhances Chemosensitivity by Directly Inhibiting SLC7A5 in Retinoblastoma. Front Oncol. 2019; 9(1163
13. Poodineh J, Sirati-Sabet M, Rajabibazl M, Mohammadi-Yeganeh S (2020) MiR-130a-3p blocks Wnt signaling cascade in the triple-negative breast cancer by targeting the key players at multiple points. Heliyon 6(11):e05434
14. Yu XF, Wang J, N OU, Guo S, Sun H, Tong J, Chen T, Li J (2019) The role of miR-130a-3p and SPOCK1 in tobacco exposed bronchial epithelial BEAS-2B transformed cells: Comparison to A549 and H1299 lung cancer cell lines. J Toxicol Environ Health A 82(15):862–869
15. Wang S, Han H, Hu Y, Yang W, Lv Y, Wang L, Zhang L, Ji J (2018) MicroRNA-130a-3p suppresses cell migration and invasion by inhibition of TBL1XR1-mediated EMT in human gastric carcinoma. Mol Carcinog 57(3):383–392
16. Lindner K, Eichelmann AK, Matuszcak C, Hussey DJ, Haier J, Hummel R. Correction: Complex Epigenetic Regulation of Chemotherapy Resistance and Biology in Esophageal Squamous Cell Carcinoma via MicroRNAs. Int. J. Mol. Sci. 2018, 19, 499. Int J Mol Sci. 2019; 20(4)

17. Jia J, Zhang X, Zhan D, Li J, Li Z, Li H, Qian J (2019) LncRNA H19 interacted with miR-130a-3p and miR-17-5p to modify radio-resistance and chemo-sensitivity of cardiac carcinoma cells. Cancer Med 8(4):1604–1618
18. Hu B, Zhang H, Wang Z, Zhang F, Wei H, Li L (2017) LncRNA CCAT1/miR-130a-3p axis increases cisplatin resistance in non-small-cell lung cancer cell line by targeting SOX4. Cancer Biol Ther 18(12):974–983
19. Eichelmann AK, Matuszcak C, Lindner K, Haier J, Hussey DJ, Hummel R (2018) Complex role of miR-130a-3p and miR-148a-3p balance on drug resistance and tumor biology in esophageal squamous cell carcinoma. Sci Rep 8(1):17553
20. Asukai K, Kawamoto K, Eguchi H, Konno M, Asai A, Iwagami Y, Yamada D, Asaoka T, Noda T, Wada H, Gotoh K, Nishida N, Satoh T, Doki Y, Mori M, Ishii H (2017) Micro-RNA-130a-3p Regulates Gemcitabine Resistance via PPARG in Cholangiocarcinoma. Ann Surg Oncol 24(8):2344–2352
21. Geng W, Ren J, Shi H, Qin F, Xu X, Xiao S, Jiao Y, Wang A (2021) RPL41 sensitizes retinoblastoma cells to chemotherapeutic drugs via ATF4 degradation. J Cell Physiol 236(3):2214–2225
22. Wang L, Sun L, Liu R, Mo H, Niu Y, Chen T, Wang Y, Han S, Tu K, Liu Q (2021) Long non-coding RNA MAPKAPK5-AS1/PLAGL2/HIF-1alpha signaling loop promotes hepatocellular carcinoma progression. J Exp Clin Cancer Res 40(1):72
23. Liang Y, Song X, Li Y, Ma T, Su P, Guo R, Chen B, Zhang H, Sang Y, Liu Y, Duan Y, Zhang N, Li X, Zhao W, Wang L, Yang Q (2019) Targeting the circBMPR2/miR-553/USP4 Axis as a Potent Therapeutic Approach for Breast Cancer. Mol Ther Nucleic Acids 17:347–361
24. Cheng R, Chen Y, Zhou H, Wang B, Du Q, Chen Y (2018) B7-H3 expression and its correlation with clinicopathologic features, angiogenesis, and prognosis in intrahepatic cholangiocarcinoma. APMIS 126(5):396–402
25. Zhong G, Lin Y, Wang X, Wang K, Liu J, Wei W (2020) H19 Knockdown Suppresses Proliferation and Induces Apoptosis by Regulating miR-130a-3p/SATB1 in Breast Cancer Cells. Onco Targets Ther 13:12501–12513
26. Wang G, Popovic B, Tao J, Jiang A (2020) Overexpression of COX7RP promotes tumor growth and metastasis by inducing ROS production in hepatocellular carcinoma cells. Am J Cancer Res 10(5):1366–1383
27. Jing J, Zhao X, Wang J, Li T (2021) Potential diagnostic and prognostic value and regulatory relationship of long noncoding RNA CCAT1 and miR-130a-3p in clear cell renal cell carcinoma. Cancer Cell Int 21(1):68
28. Zhang M, Li Q, Pan Y, Wang H, Liu G, Yin H (2018) MicroRNA-655 attenuates the malignant biological behaviours of retinoblastoma cells by directly targeting PAX6 and suppressing the ERK and p38 MAPK signalling pathways. Oncol Rep 39(4):2040–2050
29. Liu X, Li X, Li J. Long Non-coding RNA FEZF1-AS1 Promotes Growth and Reduces Apoptosis Through Regulation of miR-363-3p/PAX6 Axis in Retinoblastoma. Biochem Genet. 2021

30. Zhang HD, Jiang LH, Sun DW, Li J, Ji ZL (2017) The role of miR-130a in cancer. Breast Cancer 24(4):521–527
31. Magee P, Shi L, Garofalo M (2015) Role of microRNAs in chemoresistance. Ann Transl Med 3(21):332
32. Kong X, Zhang J, Li J, Shao J, Fang L (2018) MiR-130a-3p inhibits migration and invasion by regulating RAB5B in human breast cancer stem cell-like cells. Biochem Biophys Res Commun 501(2):486–493
33. Liu Y, Li Y, Wang R, Qin S, Liu J, Su F, Yang Y, Zhao F, Wang Z, Wu Q. MiR-130a-3p regulates cell migration and invasion via inhibition of Smad4 in gemcitabine resistant hepatoma cells. J Exp Clin Cancer Res. 2016; 35(19
34. Ouyang M, Li Y, Ye S, Ma J, Lu L, Lv W, Chang G, Li X, Li Q, Wang S, Wang W (2014) MicroRNA profiling implies new markers of chemoresistance of triple-negative breast cancer. PLoS One 9(5):e96228
35. Mi D, Carr CB, Georgala PA, Huang YT, Manuel MN, Jeanes E, Niisato E, Sansom SN, Livesey FJ, Theil T, Hasenpusch-Theil K, Simpson TI, Mason JO, Price DJ (2013) Pax6 exerts regional control of cortical progenitor proliferation via direct repression of Cdk6 and hypophosphorylation of pRb. Neuron 78(2):269–284
36. Meng B, Wang Y, Li B (2014) Suppression of PAX6 promotes cell proliferation and inhibits apoptosis in human retinoblastoma cells. Int J Mol Med 34(2):399–408
37. Bai SW, Li B, Zhang H, Jonas JB, Zhao BW, Shen L, Wang YC (2011) Pax6 regulates proliferation and apoptosis of human retinoblastoma cells. Invest Ophthalmol Vis Sci 52(7):4560–4570
38. Huang BS, Luo QZ, Han Y, Huang D, Tang QP, Wu LX (2017) MiR-223/PAX6 Axis Regulates Glioblastoma Stem Cell Proliferation and the Chemo Resistance to TMZ via Regulating PI3K/Akt Pathway. J Cell Biochem 118(10):3452–3461

Figures

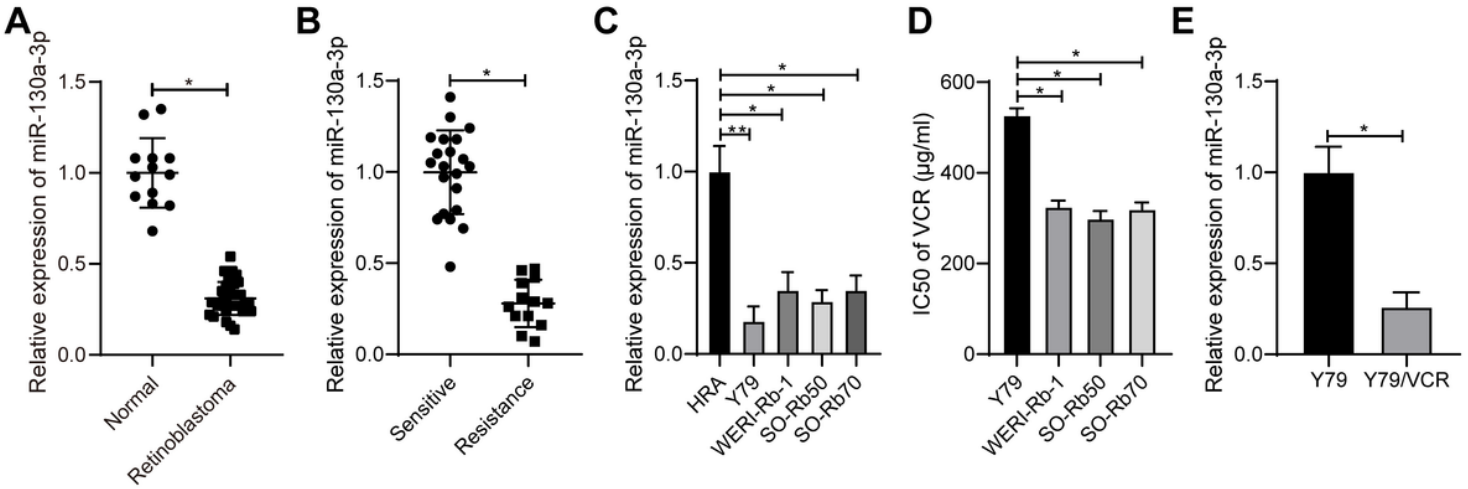

Figure 1

miR-130a-3p was downregulated in VCR-resistant RB tissues and cells. A: miR-130a-3p expression of RB tissues and normal retinal tissues was detected using RT-qPCR, normal group N = 13, RB group N = 34. B: miR-130a-3p expression of patients in the VCR-sensitive group and VCR-resistant group was detected using RT-qPCR, VCR-sensitive N = 21, VCR-resistant group N = 13. C: miR-130a-3p expression of HRA cells and RB cell lines (Y79, WERI-Rb-1, SO-Rb50, and SO-Rb70) was detected using RT-qPCR. D: The IC50 value of RB cell lines after VCR treatment was detected using CCK-8 assay. E: miR-130a-3p expression of VCR-resistant cell line (Y79/VCR) and its corresponding parental cell line (Y79) was detected using RT-qPCR. The cell experiment was repeated 3 times independently. Data were presented as mean ± standard deviation. The unpaired t test was used for comparison between two groups. One-way ANOVA was employed for the comparison among multiple groups, followed by Tukey's multiple comparisons test, *p < 0. 05.

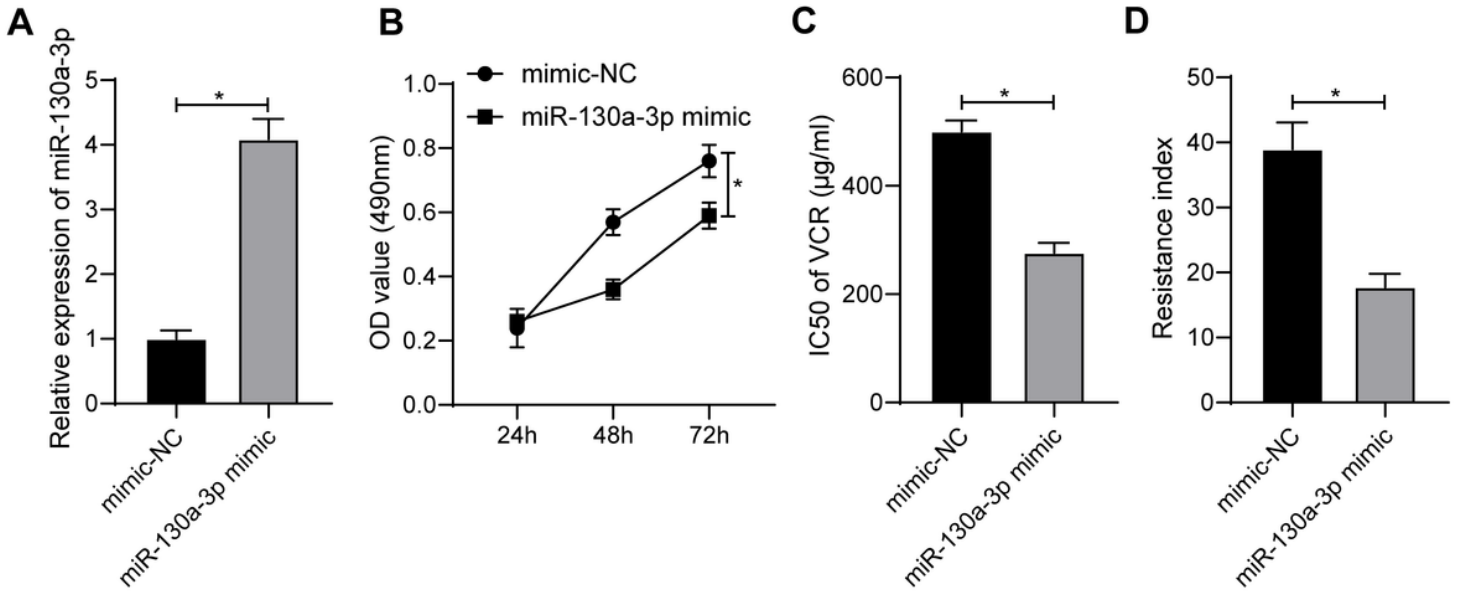

Figure 2

Overexpression of miR-130a-3p repressed the proliferation of VCR-resistant RB cells and enhanced chemosensitivity. Y79/VCR cells were transfected with miR-130a-3p mimic. A: The transfection efficiency was verified using RT-qPCR. B: The cell proliferation was measured using MTT assay. C: The IC50 value of cells in each group was detected using CCK-8 assay. D: The resistance index of cells in each group was detected using CCK-8 assay. The cell experiment was repeated 3 times independently. Data were presented as mean ± standard deviation. The unpaired t test was used for comparison between two groups, *p < 0. 05.

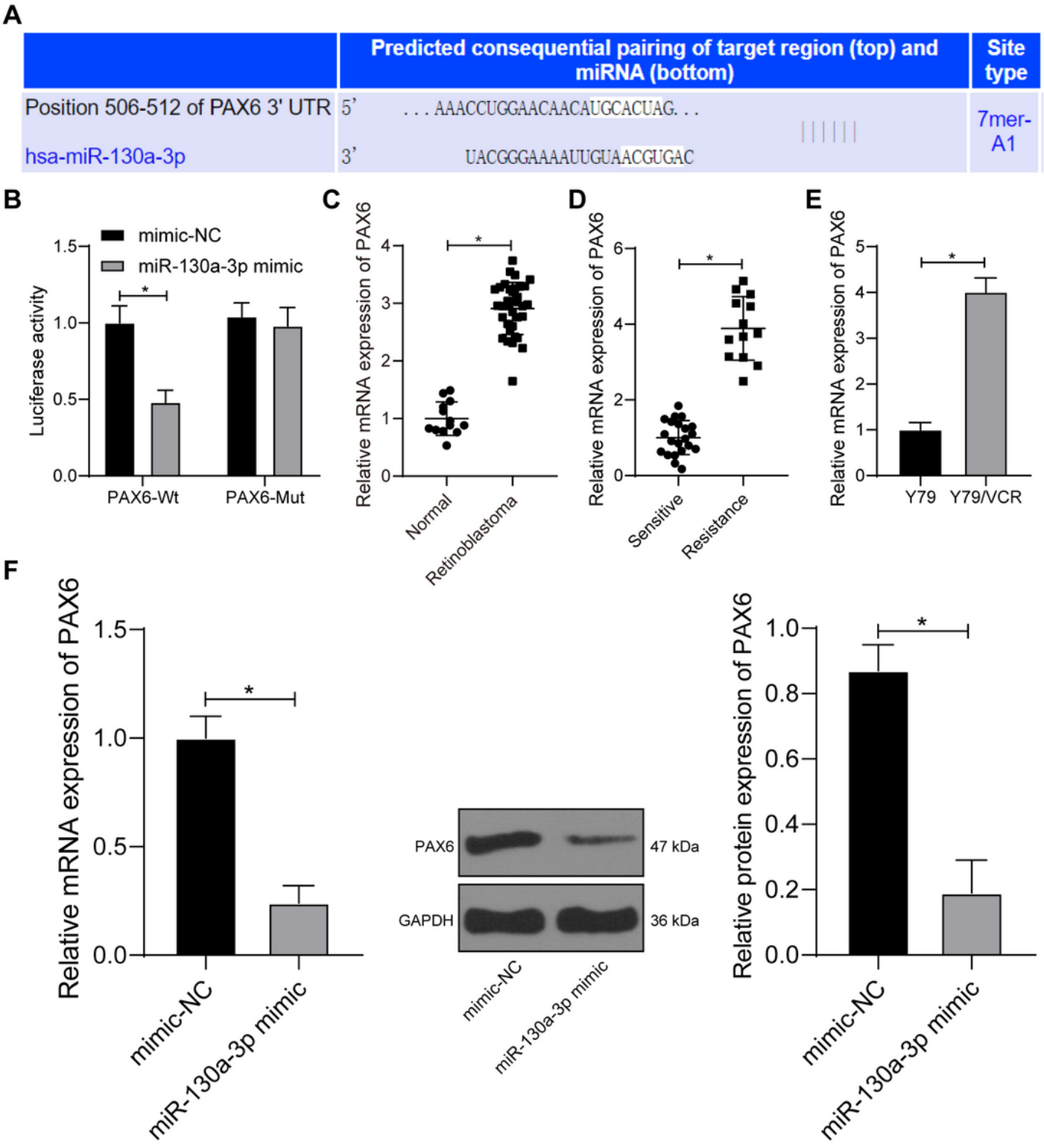

Figure 3

miR-130a-3p targeted PAX6 expression. A: The binding site of miR-130a-3p and PAX6 was predicted through Targetscan. B: The targeting relationship between miR-130a-3p and PAX6 was verified using dual-luciferase assay. C: PAX6 expression of RB tissues and normal retinal tissues was detected using RT-qPCR, normal group N = 13, RB group N = 34. D: PAX6 expression of VCR-resistant RB tissues and VCR-sensitive RB tissues was detected using RT-qPCR. E: PAX6 expression of VCR-resistant cell line (Y79/VCR)

and its corresponding parental cell line (Y79) was detected using RT-qPCR. F: PAX6 expression of Y79/VCR cells after overexpression of miR-130a-3p was detected using RT-qPCR. The cell experiment was repeated 3 times independently. Data were presented as mean ± standard deviation. The unpaired t test was used for comparison between two groups. One-way ANOVA was employed for the comparison among multiple groups, followed by Tukey's multiple comparisons test, *p < 0. 05.

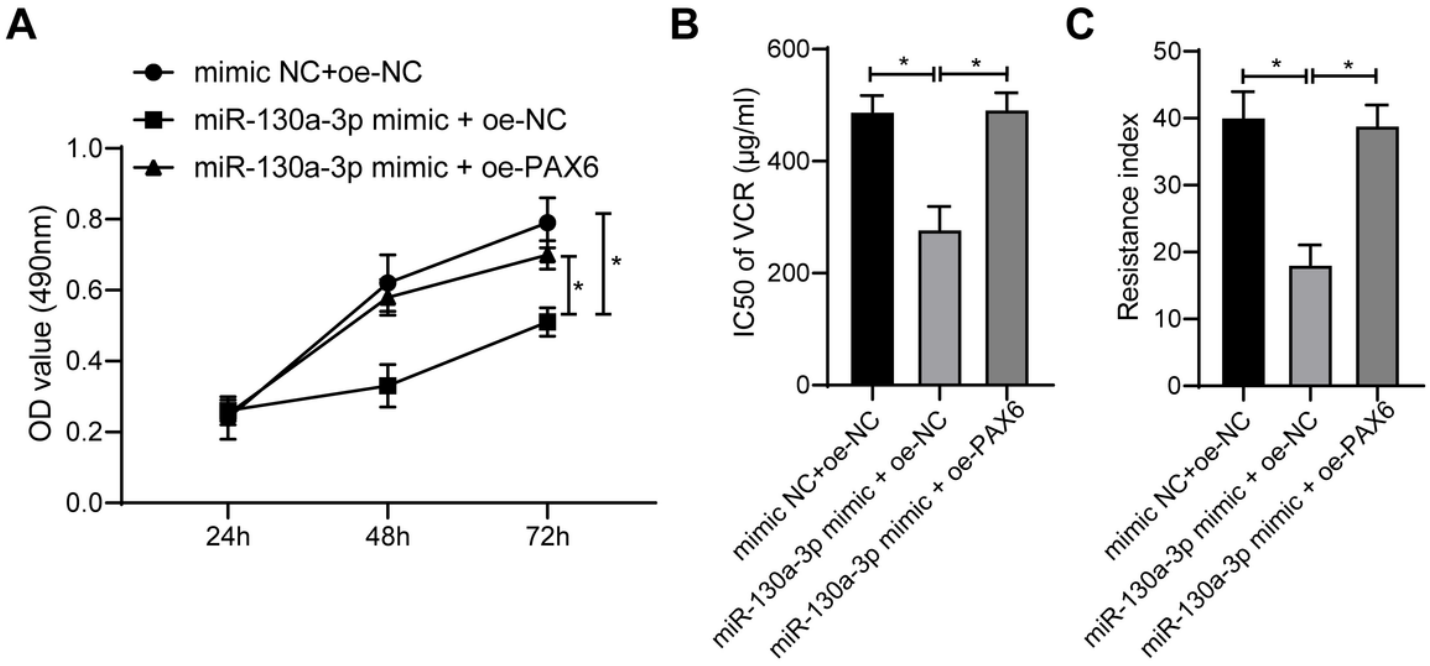

Figure 4

Overexpression of PAX6 reversed the effect of miR-130a-3p on chemosensitivity of RB. miR-130a-3p and PAX6 were overexpressed in Y79/VCR cells. A: The cell proliferation was measured using MTT assay. B: The IC50 value of cells in each group was detected using CCK-8 assay. C: The resistance index of cells in each group was detected using CCK-8 assay. The cell experiment was repeated 3 times independently. Data were presented as mean ± standard deviation. One-way ANOVA was employed for the comparison among multiple groups, followed by Tukey's multiple comparisons test, *p < 0. 05.

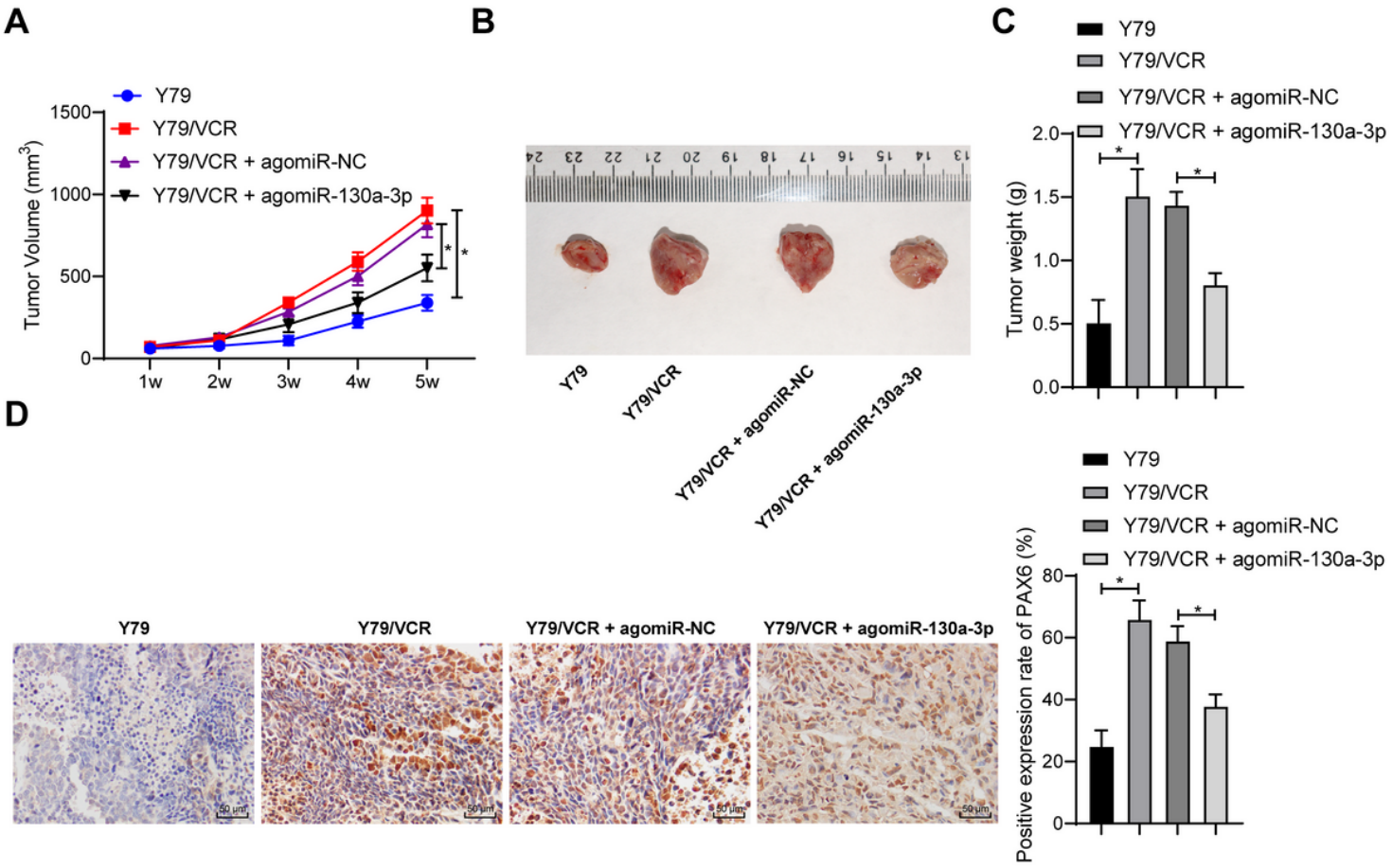

Figure 5

Overexpression of miR-130a-3p suppressed tumor growth and reduced VCR resistance in vivo. A: Tumor growth curve of nude mice in each group. B: Representative images of tumors in each group. C: Statistical analysis of tumor weight in each group. D: The positive expression rate of PAX6 was detected using immunohistochemistry. N = 8. Data were presented as mean ± standard deviation. Data in panel A were analyzed using repeated measure ANOVA, and data in panels C/D were analyzed using one-way ANOVA, followed by Tukey's multiple comparisons test, *p < 0. 05.